Measurements of Backscatter Phase Function and Depolarization in Cirrus Clouds made with the University of Wisconsin High Spectral Resolution Lidar.

E. W. Eloranta*, R. E. Kuehn and R. E. Holz
University of Wisconsin, 1225 W. Dayton Street, Madison, Wisconsin 53706, USA
Phone: 608-262-7327 Fax: 608-262-5974, Email: eloranta@lidar.ssec.wisc.edu

January 2, 2001

1 Introduction

Cirrus clouds play an important role in the earth's radiation balance. Additional data on the optical properties of these clouds is required for climate modeling. The University of Wisconsin High Spectral Resolution Lidar (HSRL) measures optical depth, backscatter cross section and depolarization. The HSRL separates the molecular backscatter from aerosol and cloud backscatter. The separated molecular backscatter is used as a known target to provide an absolute calibration of the measurements. This paper will present simultaneous measurements of backscatter phase function and depolarization in cirrus clouds.

2 Observations

During 1994, the HSRL was operated in conjunction with the evening overpass of the NOAA polar orbiter. Data was collected on nearly every evening when cirrus was visible over Madison, Wisconsin. To minimize noise the HSRL data was averaged over 3 minute time intervals and 165m altitude layers. Data points were selected to include only points with a statistical error of less than 5%. Only points with a measured depolarization of greater than 20% were selected to insure that the cloud consisted of ice crystals. In addition only uniform sections of the cloud were selected for analysis to prevent errors due to averaging between cloudy and clear parcels. Uniform cloud parcels were selected by limiting the analysis to those points where the backscatter of the point did not vary by more than 15% from adjacent points. Figure 1 shows the distribution of backscatter phase function values computed in this manner. It shows a prominent peak at $\mathcal{P}(180)/4\pi \approx .04$.

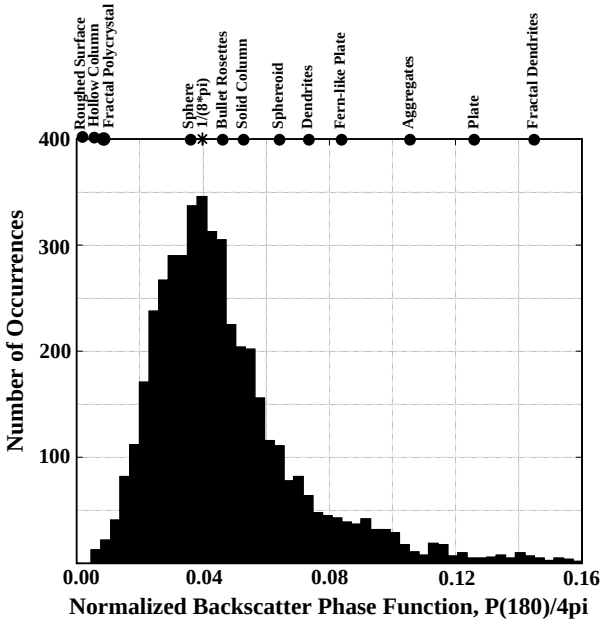

Figure 1: Number of occurrences of a given value of the backscatter phase function. Backscatter phase functions generated from ray tracing solutions are shown above the figure. Ray tracing values were supplied by Ping Yang (personal communication).

It is interesting to note that this is the value which would be expected for a particle whose phase function consisted of a diffraction peak containing 1/2 of the scattered energy with the rest of the energy scattered isotropically. This particle would have a backscatter phase function, $\mathcal{P}(180)/4\pi = 1/8\pi = .0398$.

It is significant that values of the backscatter phase function computed by ray tracing for various geometrically perfect crystal types would suggest a much wider distribution of values. However, ice crystals collected from clouds seldom consist of single crystal type and few natural crystals exhibit the perfect symmetries of the model crystals.

Figure 2 presents a plot of the depolarization as function of backscatter cross section measured for the 1994 data set. Notice that the depolarization appears to increase with increasing backscatter cross section. This can be explained by differences between external and internal reflections from the ice crystals. External reflections from facets which return energy to the receiver must occur from facets which are oriented normal to the lidar beam. These reflections do not affect the polarization and the facets are not very efficient reflectors because the Fresnel reflectivity of ice is low. Internal corners are efficient reflectors and the light rays must enter and leave the crystal through a tilted surface which induces depolarizations. Consequently, because the fraction of the scattering from internal corners and external facets will be a function of crystal morphology, we can expect that the depolarization and the backscatter phase function will be correlated.

Despite the stringent selection process used to select data points for inclusion in figure 1, we were concerned about errors in the derivative, $\frac{d\tau}{dz}$ which is sensitive to noise. To increase our confidence, we hand picked 34 cirrus clouds from the data set. These were selected for uniformity such that we could form long time averages without introducing errors due to averaging over inhomogeneities. To minimize noise in the derivative we have calculated the bulk value of the backscatter phase function averaged through the cloud. Here the backscatter phase function is computed from the integral of the backscatter cross section through the cloud and the optical depth of the cloud. Figure 3 describes the process used to compute the bulk phase function. The simple optical depth $\tau(Ro, R)$ is computed from the molecular signal, Nm(R) and the air density profile, $M\rho(R)$.

$$\tau(Ro, R) = \frac{1}{2} ln[\frac{M\rho(R)}{Nm(R)}] - \frac{1}{2} ln[\frac{M\rho(Ro)}{Nm(Ro)}] \quad (1)$$

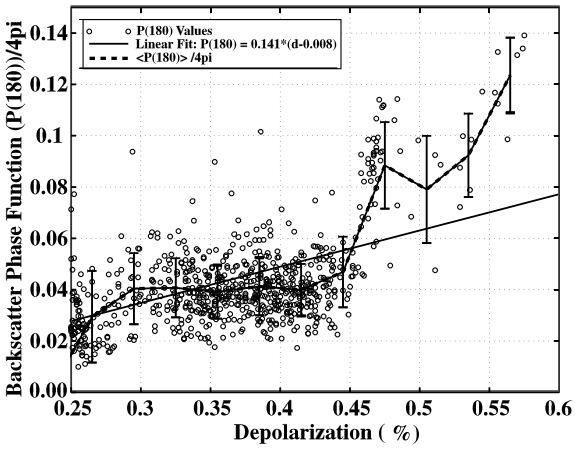

Figure 2: Backscatter phase function as a function of depolarization.

Where Ro is the base of the cloud and R is the top. The integrated aerosol backscatter cross section, B, was then computed from β.

$$B(Ro, R) = \int_{Ro}^{R} \beta(x) dx \quad (2)$$

The bulk backscatter phase function, $\frac{\mathcal{P}(180)}{4\pi}$, was then determined using equation 3.

$$\tau(Ro, R) \frac{\mathcal{P}(180)}{4\pi} = B(Ro, R) \quad (3)$$

The point R_t is chosen well above the cloud top. This reduces multiple scattering errors because most multiple small angle forward scattering from the cloud will have escaped from the 160μrad receiver field of view before reaching R_t. Figure 3 provides a sample comparison of $\tau(R_0, R)$ and $B(R_0, R)\frac{4\pi}{\mathcal{P}(\infty \forall I)}$.

Figure 4 shows the bulk backscatter phase function distribution computed from the 34 unifrom cirrus clouds from the 1994 and 1995 data set. The bulk backscatter phase funtion disturbution shows a prominent peak at $\mathcal{P}(180)/4\pi \approx .04$. This agrees with the backscatter phase function probability computed

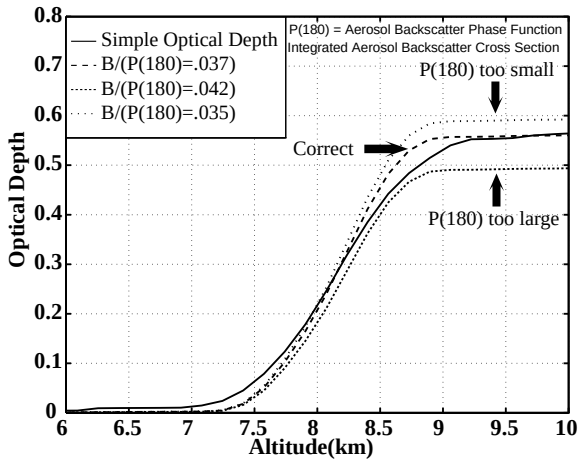

Figure 3: Calculation of the bulk backscatter phase-function. The bulk $\mathcal{P}(180)/4\pi$ is adjusted until $\frac{\mathcal{P}(180)}{4\pi}\tau(Ro,R)$ = B(Ro,R)

through out the cloud in figure 1. We carefully examined data from the cloud with a bulk $\mathcal{P}(180)/4\pi \approx 0.088$ in figure 4 and could not identify any source of error which could cause it to deviate so much from the dominate peak. Thus, it must represent scattering from a less frequent crystal type. This also leads to the conclusion that the occurrences of large backscatter phase functions in figure 1 are also likely to reflect variability in crystal morphology rather than experimental error.

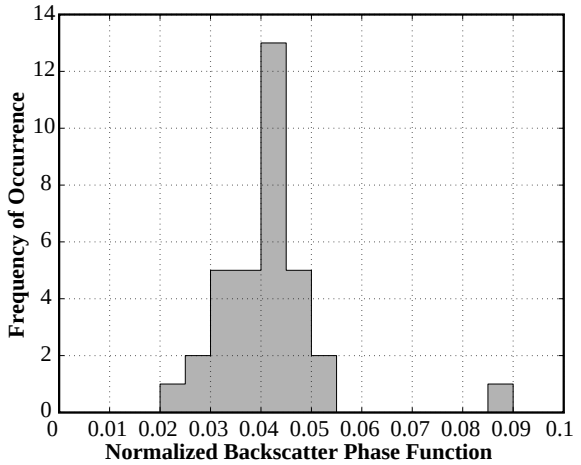

Figure 4: Histogram of cloud layer average backscatter phase functions.

3 Acknowledgments

The 1994 HSRL data was collected by Paivi Pirronen. Funding for this research was provided by National Science Foundation Grant ATM-9321330 and Air Force contract F19628-96-C-0097.